Defect perception thresholds on specular surfaces

Mathias Ziebarth

Vision and Fusion Laboratory
Institute for Anthropomatics and Robotics
Karlsruhe Institute of Technology, Germany
mathias.ziebarth@kit.edu

Technical Report IES-2014-11

Abstract: Today, measurement methods like deflectometry allow accurate measurements of specular surfaces. The measurement methods are often more precise than human vision. If the aim is to inspect surfaces for defects that would disturb humans, so called aesthetic defects, it is important to understand the connection between the measurement method and human vision. This problem is addressed in this report. In contrast to matte surfaces, there are different influencing factors for the perception of specular surfaces. We are proposing a model which introduces a lower bound for the visibility of defects on specular surfaces. This means that defects smaller than this bound cannot be identified by an average human observer.

1 Introduction

The automated visual inspection of specular surfaces is a practical problem with many applications. Today, there are methods known to get precise measurements of specular surfaces, ranging from small glossy mobile devices up to large lacquered automobile bodies. One way to acquire the surface shape is a measurement method called deflectometry, which can be used for specular to partially specular surfaces. It has the advantage of being especially sensitive to changes in the surface gradient. This corresponds to the human perception of specular surfaces. When surfaces which have to "look good" are inspected, all defects visible to a human under defined conditions should be detected. Therefore the defects are defined by some aesthetical measure, which depends on the human visual system, surface properties and a typical environment. In this paper we propose such an approach to quantify the visibility of aesthetic defects. For this purpose we define thresholds for the visibility of defects on specular surfaces. Defects smaller than these quantifications are invisible for an average human observer.

2 Related Work

Some work was done to automatically assess specular surfaces as humans would do. First of all, Hsakou [Hsa06] uses deflectometry and makes use of the surface curvature for assessment, as it correlates to human visual inspection. Additional decision criteria like location, area, amplitude and density are identified by comparing automated with manual inspections. Finally, tolerance thresholds for combinations of the identified criteria are chosen assisted by an inspector.

The detection, classification and evaluation of surface defects is a rather general task with many applications and accordingly a lot of studies exist in this field. The studied applications range from the evaluation of auto-body panels [And09, Fer13], assessing scratch damages in bulk materials and coatings [HWP03], scratch visibility on polymers [RSW+03, JBH+10, LBS+11] and defects on machined and painted surfaces [PK06].

3 Derivation of the model

In this section we derive the model which connects the influencing factors with the minimum defect sizes visible for a human observer.

3.1 Resolution on the surface

Given the variables angular resolution θ, incident angle on the surface α and the viewing distance to the surface d we want to determine the resolution on the surface a as shown in Fig. 3.1:

$$\frac{a}{\sin(\theta)} = \frac{d'}{\sin(\alpha')}, \tag{3.1}$$

$$\alpha' = \alpha - \frac{\theta}{2}, \tag{3.2}$$

$$\frac{d'}{\sin(\alpha)} = \frac{d}{\sin(180 - \alpha - \frac{\theta}{2})}.$$

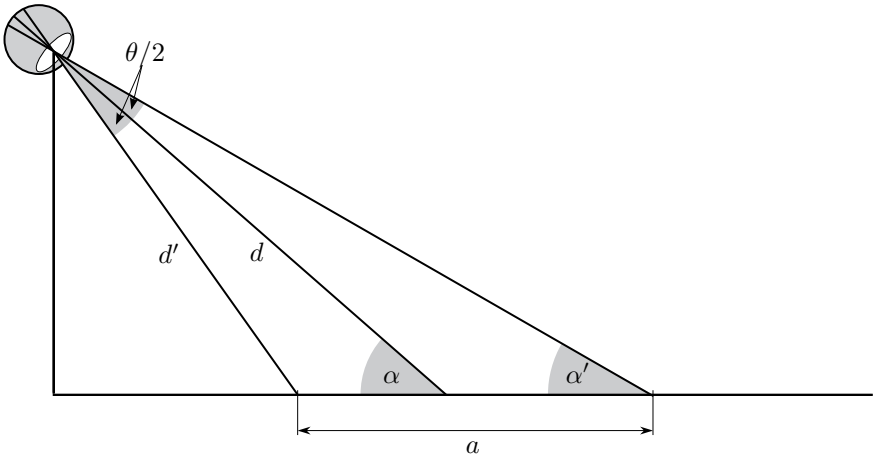

Figure 3.1: Lateral resolution on the surface.

Using the symmetry of the sine function $\sin(180 - x) = \sin(x)$ we get

$$d' = \frac{d\sin(\alpha)}{\sin(\alpha + \frac{\theta}{2})}. \tag{3.3}$$

Inserting (3.2) and (3.3) in (3.1) we obtain

$$a = \frac{d\sin(\theta)\sin(\alpha)}{\sin(\alpha - \frac{\theta}{2})\sin(\alpha + \frac{\theta}{2})}. \tag{3.4}$$

Using the sinus law $\sin(x)\sin(y) = \frac{1}{2}(\cos(x-y) - \cos(x+y))$ and the asymmetry of the cosine function $\cos(x) = \cos(-x)$ (3.4) can be simplified to

$$a = 2d\frac{\sin(\theta)\sin(\alpha)}{\cos(\theta) - \cos(2\alpha)}. \tag{3.5}$$

In the special case of $\alpha = 90$ (3.5) simplifies to

$$\begin{aligned} a &= 2d\frac{\sin(\theta)}{\cos(\theta) + 1} \\ &= 2d\tan(\frac{\theta}{2}). \end{aligned}$$

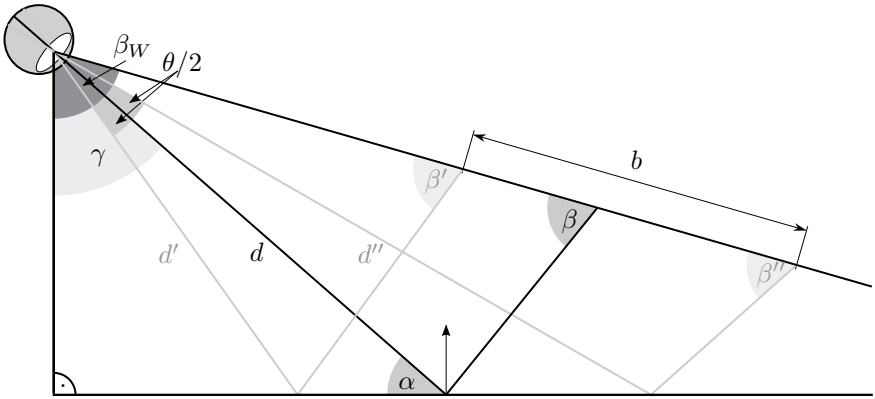

Figure 3.2: Angular resolution caused by resolution on the screen.

3.2 Resolution on the screen

Similar to section 3.1 in (3.5) and using the variables angular resolution θ, incident angle on the screen β and the viewing distance from the observer over the surface to the screen $d + h$ we determine the resolution on the screen b as in Fig. 3.2:

$$b = 2(d + h)\frac{\sin(\theta)\sin(\beta)}{\cos(\theta) - \cos(2\beta)}. \tag{3.6}$$

In the special case of $\beta = 90$ (3.6) simplifies to

$$b = 2(d + h)\tan(\frac{\theta}{2}).$$

3.3 Deflection on the screen

Similar to the previous sections 3.1 and 3.2 as in (3.5) and (3.6) and using the variables surface normal change $\Delta\phi$, incident angle on the screen β and the distance from the surface to the screen h we determine the deflection of the viewing rays on the screen c as in Fig. 3.3:

$$c = 2h\frac{\sin(\Delta\phi)\sin(\beta)}{\cos(\Delta\phi) - \cos(2\beta)}. \tag{3.7}$$

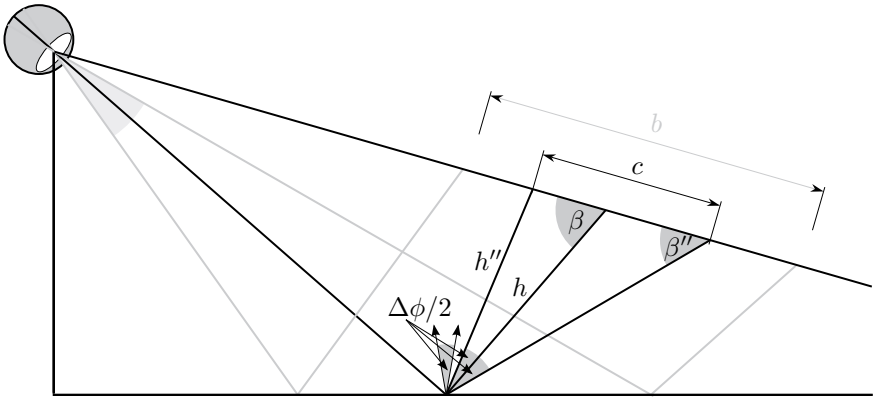

Figure 3.3: Deflection on the screen caused by change of the surface normal.

In the special case of $\beta = 90$ (3.7) simplifies to

$$c = 2h \tan(\Delta\phi).$$

3.4 Defect model triangle

Assuming a triangular shaped defect as in Fig. 3.4, we need the variable $\Delta\phi$ for the triangle gradient and a_t for the lateral extend of the defect to obtain the defect depth t

$$a_t = \frac{t}{\tan(\frac{\Delta\phi}{2})}. \tag{3.8}$$

3.5 Deviation

A defect on the surface is visible if two conditions are met. At first the observer has to be able to resolve the defect on the surface $a = a_t$ using (3.5) and (3.8), which leads to

$$2d\frac{\sin(\theta)\sin(\alpha)}{\cos(\theta) - \cos(2\alpha)} = \frac{t}{\tan(\frac{\Delta\phi}{2})}. \tag{3.9}$$

In the special case of $\alpha = \beta = 90$ (3.9) simplifies to

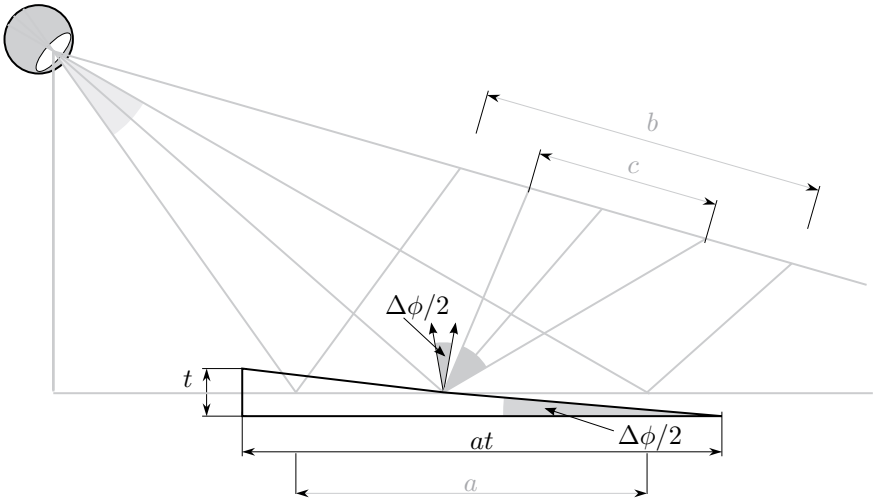

Figure 3.4: Triangular defect model causes deflection of viewing rays.

$$2d\tan(\frac{\theta}{2}) = 2h\tan(\Delta\phi). \tag{3.10}$$

The second condition is that the deflection has to be resolved on the screen $b = c$ using (3.6) and (3.7)

$$2(d+h)\frac{\sin(\theta)\sin(\beta)}{\cos(\theta)-\cos(2\beta)} = 2h\frac{\sin(\Delta\phi)\sin(\beta)}{\cos(\Delta\phi)-\cos(2\beta)}. \tag{3.11}$$

In the special case of $\alpha = \beta = 90$ (3.11) simplifies to

$$2(d+h)\tan(\frac{\theta}{2}) = 2h\tan(\Delta\phi),$$

which leads to

$$\Delta\phi = \arctan(\frac{d+h}{h}\tan(\frac{\theta}{2})). \tag{3.12}$$

Inserting (3.12) into (3.10) we get

$$2(d+h)\tan(\frac{\theta}{2}) = \frac{t}{\frac{d+h}{h}\tan(\frac{\theta}{2})}$$

and hence

$$t = 2(d+h)\frac{d}{h}\tan^2(\frac{\theta}{2}).$$

As it can be observed that the angle $\Delta\phi$ is nearly 0, we can approximate $\tan(\Delta\phi) \approx \Delta\phi$, so analogue to (3.12) we can write $\Delta\phi$ without assuming $\alpha = \beta = 90$ as

$$\Delta\phi = \frac{2\sin^2(\beta)(d+h)\sin(\theta)}{(d+h)\sin(\theta) - h\cos(2\beta) + h\cos(\theta)}. \tag{3.13}$$

Inserting (3.13) into (3.5) and using the triangle defect model from (3.8) we get

$$t = -\frac{2d\sin(\alpha)\sin(\theta)\tan\left(\frac{\sin^2(\beta)(d+h)\sin(\theta)}{(d+h)\sin(\theta)-h\cos(2\beta)+h\cos(\theta)}\right)}{\cos(2\alpha)-\cos(\theta)}. \tag{3.14}$$

The proposed model (3.14) gives the lower bound for the visibility of a defect on a specular surface. For the defect we assume a triangular shape (3.8) that deflects one viewing ray on a screen. With an appropriate pattern this deflection can be resolved. Furthermore the defect itself has to be large enough to be resolved on the surface, as given in (3.5).

4 Results & Discussion

Before evaluating the model derived above, it is necessary to define the viewing capabilities of an average human observer and a typical surrounding. We describe the viewing capability with the angular resolution of the human eye and assume an observer with the average visual acuity of $\theta = \frac{1}{60}^\circ$ [PPBS08]. The visual acuity describes the spatial resolution of the human eye, especially the ability to discriminate between two separate points. Furthermore as typical environment for the observation we have chosen a car dealership with viewing distances ranging from $d_{\text{min}} = \frac{30}{100}m$ to $d_{\text{max}} = 2m$ and screen distances ranging from $h_{\text{min}} = 1m$ to $d_{\text{max}} = 10m$. The screen has to show patterns that allow the detection of very small deflections of viewing rays.

As a first result, Figure 4.1 shows the minimal visible width by evaluating (3.5) with $\alpha = 90$. Figure 4.2 shows the minimal visible height by evaluating (3.14) with $\alpha = \beta = 90$ and Figure 4.3 shows the minimal visible height by evaluating (3.14) with minimal viewing distance d_{min} and maximal screen distance h_{max}.

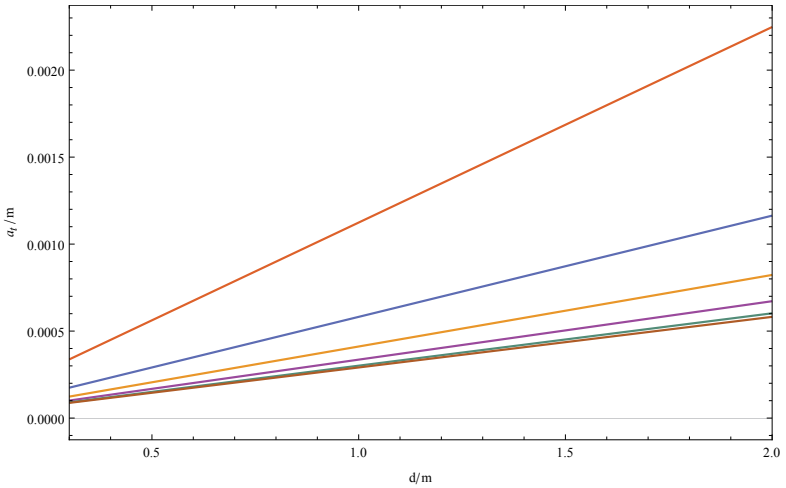

Figure 4.1: Minimal visible defect width a_t with respect to viewing distance d for several incident angles on the surface α.

Looking at (3.14) it can be seen that for minimal viewing distance d_{min} and maximal screen distance h_{max} the smallest defects are visible. Under these optimal viewing conditions, a defect may be as small as $87\mu m$ in lateral extend, 0.01 steepness and $32nm$ in height. One drawback of the model is that the lateral extend and steepness of the defect are linked. Thus defects with the same height have a larger gradient when their lateral extend is smaller, which does not correspond to the intuition that small changes in height are better visible when the defect has a large extend. Another drawback is that we only look at the first derivative of the surface, which is responsible for the deviation of single viewing rays. Usually humans are used to observe distortions of known patterns, which corresponds to the second derivative of the surface. Also it results in reducing the capabilities of the human eye to just one value, the visual acuity. Areal pattern resolution capabilties are ignored.

5 Conclusion

We proposed a model to estimate lower bounds for the visibility of defects on specular surfaces. Therefore a perfect specularity, a triangle shaped defect and an optimal pattern on the screen were assumed. The benefit of the model is that the visibility is attributed to known quantities such as the visual acuity of the human

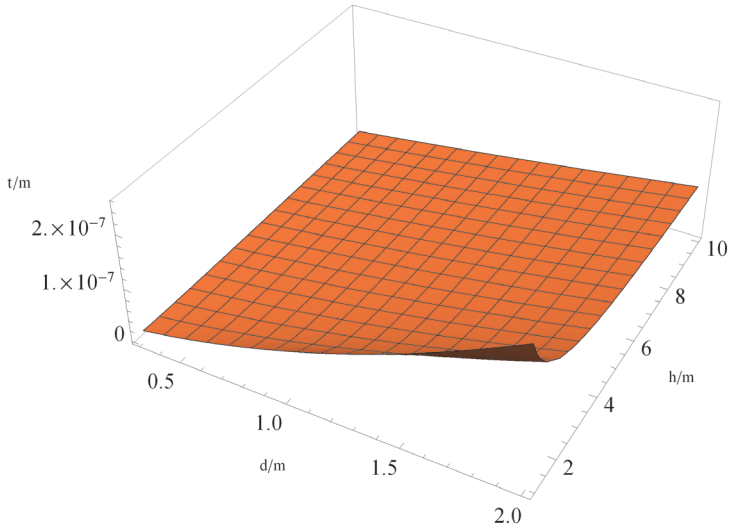

Figure 4.2: Minimal visible defect height with respect to viewing distance d and screen distance h and incident angles on the surface and the screen of $\alpha = \beta = 90$.

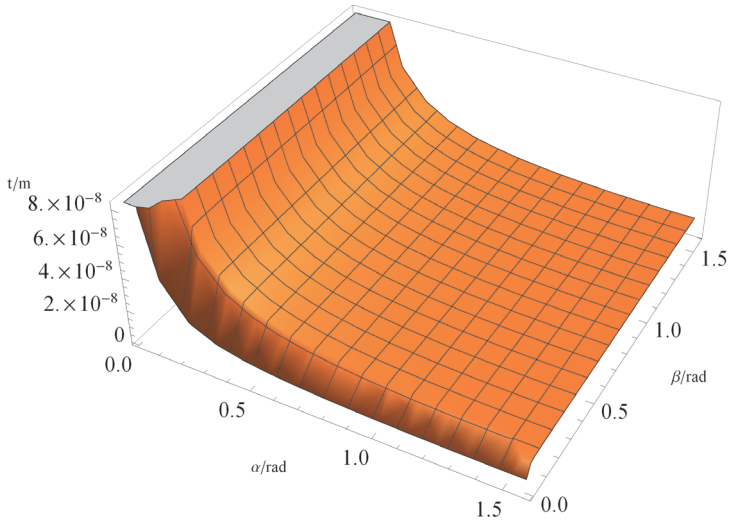

Figure 4.3: Minimal visible defect height with respect to incident viewing angle α and screen angle β and for minimal viewing distance d and maximal screen distance h.

eye, observation angles and distances. Assuming an average acuity under optimal viewing conditions the model gives very small lower boundaries for the visibility of defects. The lower bounds obtained with this model are very small, but as the model makes some artificial worst case assumptions such as a perfect specular surface and a perfect pattern, the results should get more practical as more realistic assumptions are included in the model.

Bibliography

[And09] A. Andersson. Evaluation and visualisation of surface defects on auto-body panels . *Journal of Materials Processing Technology*, 209(2):821–837, 2009.

[Fer13] K. Fernholz. Quantifying the Visibility of Surface Distortions in Class "A" Automotive Exterior Body Panels. *Journal of Manufacturing Science and Engineering*, 135:011001–1, 2013.

[Hsa06] Réda Hsakou. Curvature: the relevant criterion for class-a surface quality. *JEC Composites Magazine*, pages 105–108, March 2006.

[HWP03] I. Hutchings, P. Wang, and G. Parry. An optical method for assessing scratch damage in bulk materials and coatings. *Surface and Coatings Technology*, 165(2):186–193, 2003.

[JBH+10] H. Jiang, R. Browning, M. Hossain, H-J. Sue, and M. Fujiwara. Quantitative evaluation of scratch visibility resistance of polymers. *Applied Surface Science*, 256(21):6324–6329, 2010.

[LBS+11] P. Liu, R. Browning, H-J. Sue, J. Li, and S. Jones. Quantitative scratch visibility assessment of polymers based on Erichsen and ASTM/ISO scratch testing methodologies. *Polymer Testing*, 30(6):633–640, 2011.

[PK06] F. Puente León and S. Kammel. Inspection of specular and painted surfaces with centralized fusion techniques. *Measurement*, 39(6):536–546, 2006.

[PPBS08] F. Pedrotti, L. Pedrotti, W. Bausch, and H. Schmidt. *Optik für Ingenieure*. Springer Berlin Heidelberg, 2008.

[RSW+03] P. Rangarajan, M. Sinha, V. Watkins, K. Harding, and J. Sparks. Scratch visibility of polymers measured using optical imaging. *Polymer Engineering & Science*, 43(3):749–758, 2003.